

## Chapter 2

# The Practical Implications of Bubble Formation in Conventional Water Treatment

Paolo Scardina and Marc Edwards

**Abstract.** Air entrainment and ozonation are the key causes of dissolved gas supersaturation and eventual bubble formation in water treatment plants. Total dissolved gas probes (TDGP) are now available to directly measure supersaturation and have many advantages compared to conventional techniques. Bubble formation during coagulation-flocculation hindered particle sedimentation, producing settled turbidities double that of solutions without dissolved gases. In a filtration study, run time to one half of initial flow was decreased by 54% when the source water was increased from 0.1 to 0.2 atm supersaturation. Indeed, even at 0.05 atm supersaturation, run length was only 21 hours in solutions without added particulate matter. A case study confirmed that bubble formation can interfere with coagulation and filtration processes at conventional treatment plants.

### Introduction

Dissolved gas supersaturation can lead to air bubble formation in water treatment plants and cause some unusual problems. Treatment plant operators have long suspected that bubble formation hinders particle agglomeration and can even float flocs during conventional coagulation-flocculation-sedimentation, thereby overloading filters. Bubbles forming inside filters also hinder performance by creating unwanted headloss—a phenomenon commonly termed “air binding.”<sup>1</sup> Finally, air bubbles in water have been reported to measure as turbidity<sup>2</sup>, and filter media loss is believed to occur from bubble release during backwashing.

Although these problems routinely affect water utilities such as Metropolitan Water District, City of Myrtle Beach, and Boulder, Colorado, very little fundamental research has been aimed at confirming, understanding, or eliminating this common problem. The goal of this paper is to discuss practical situations that lead to bubble formation at water treatment plants, to illustrate how bubble formation can affect treatment processes such as coagulation and filtration, and to confirm some key predictions in a case study.

## Bubble Formation and Dissolved Gas Supersaturation

Bubbles can form whenever the activity of dissolved gas(es) in solution—as measured by partial pressure—exceeds the ambient hydrostatic pressure.

$\Sigma \text{Dissolved Gas(es) Partial Pressure} > \text{Ambient Hydrostatic Pressure} \rightarrow \text{Bubble Formation}$

Since it is believed that water treatment plants typically operate as closed systems,<sup>3</sup> bubble formation might be the preferred means of alleviating dissolved gas supersaturation, rather than interfacial transfer. The mechanism by which bubbles are expected to form at utilities is heterogeneous nucleation—dissolved gases diffuse into air cavities (nucleation sites) located on imperfections of solid surfaces.<sup>4</sup> As supersaturated dissolved gas diffuses into the nucleation site, the air cavity grows and eventually creates a bubble which can detach.

Waters can become supersaturated through a number of processes (Table 1), although the most common seem to be either air entrainment or ozonation. Air can be entrained in pipelines during cascading or turbulent conditions at the source water intake or through drawing of air into pipes at exhausts ports by excessive pipe flow velocities (Figure 1). Increased hydrostatic pressure in the pipeline drives subsequent gas dissolution, especially when there are large elevation differences between the source and the utility (1800 feet at Boulder, CO). This entrained air is then released in the form of bubbles when it enters the treatment plant. Greater hydrostatic pressures and quantities of entrained air can increase the degree of gas supersaturation.

Ozonation can either increase or decrease gas supersaturation, depending on the specific circumstances. In general, gas diffusion at depth in a contact chamber will directly cause supersaturation of ozone even assuming it does not react or degrade (Figure 2). With air as the carrier gas, the partial pressures of all atmospheric gases will increase, while oxygen saturation increases and other gases are stripped in situations if a pure oxygen carrier gas is used. Supersaturation will tend to increase with depth of bubble injection and increased airflow due to the additional hydrostatic pressure and the added air-water contact time.

Table 1 – Sources of Dissolved Gas Supersaturation

Source	Key Reaction
Air Entrainment	$[G] = k_h * \rho G$ : Increased partial pressure at depth
Ozonation <sup>5</sup>	$O_3 \rightarrow O_2$ , $[G] = k_h * \rho G$ : 1 mole of $O_3$ can degrade to 1 mole $O_2$ , and increase of carrier gas partial pressure at depth
Coagulant Addition	$[HCO_3^-] + [H^+] \rightarrow [H_2CO_3]$ : Acidic coagulants convert alkalinity to carbon dioxide
Lake/Reservoir Aeration, $CO_2$ Addition, Dissolved Air Flotation	$[G] = k_h * \rho G$ : Increased partial pressure at depth
Photosynthesis and Anaerobic Growth	$106CO_2 + 16NO_3^- + HPO_4^{2-} + 122H_2O + 18H^+ \rightarrow C_{106}H_{263}O_{110}N_{16}P + 138O_2$ (Algae Photosynthesis <sup>6</sup> ) Microbial and algae growth can potentially supersaturate waters
Hypochlorite <sup>7</sup>	$H^+OCl + H^+OCl \rightarrow O_2 + 2HCl$ , Hypochlorite disinfectant can degrade to form $O_2$
Thermal Warming	$[G] = k_h * \rho G$ : Waters hold less gas at increased temperatures
Barometric Pressure Change	$[G] = k_h * \rho G$ : Waters hold less gas at lower barometric pressures

Ozone can also directly cause supersaturation by chemical degradation to oxygen at a molar ratio of one oxygen to one ozone.<sup>5</sup> For example, consider a water at equilibrium with a 2% ozone and 98% oxygen gas phase at 1 atm. After the ozone completely degrades to oxygen at 25 °C, the solution would then be supersaturated 0.18 atm with pure oxygen. Finally, ozonation can actually decrease dissolved gas supersaturation if the water is already highly saturated, since the injected bubbles provide for more rapid release of supersaturated gas transfer than is possible through heterogeneous nucleation. A pilot study for the City of San Diego found 67% reductions in headloss buildup, due to reduced air binding from ozonation prior to filtration.<sup>8</sup>

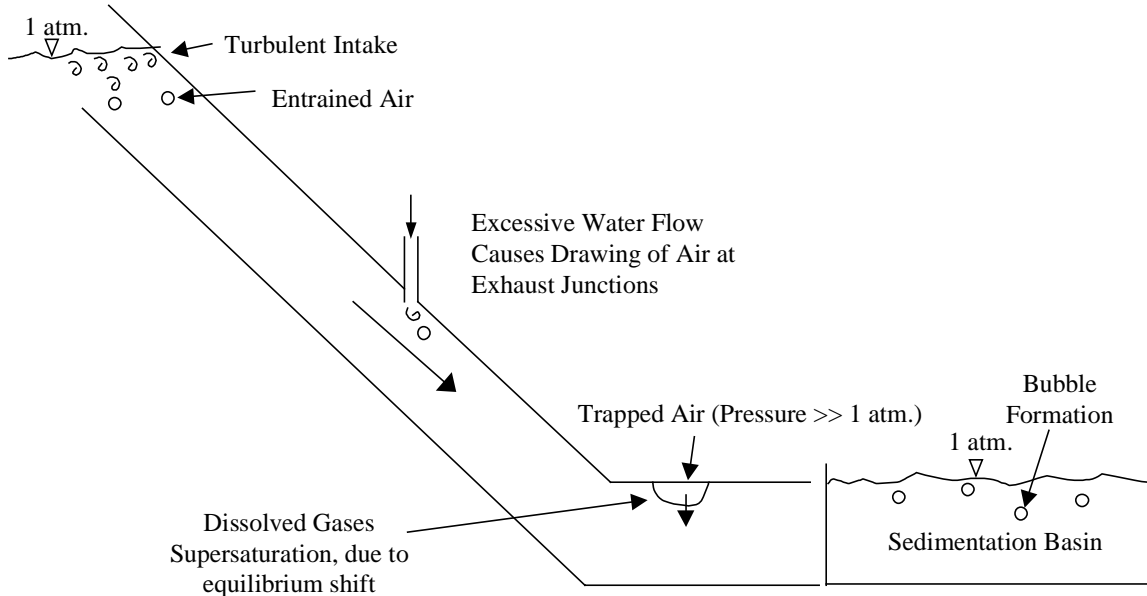


Figure 1 – Dissolve Gas Supersaturation from Source Water Air Entrainment

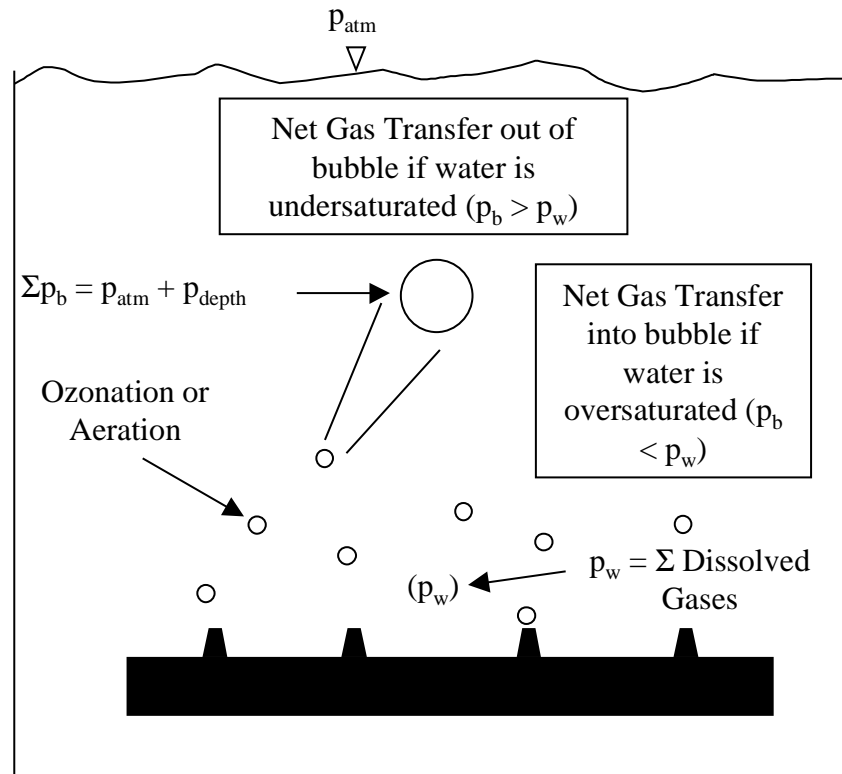


Figure 2 – The Effects of Ozonation on the Dissolved Gas Saturation

Lake or reservoir aeration, carbon dioxide gas injection, and dissolved air flotation can supersaturate waters through mechanisms similar to ozonation by diffused injection at depth. Although carbon dioxide is not commonly considered a factor in bubble formation, coagulant addition can cause bubble formation by converting bicarbonate alkalinity to supersaturated carbon dioxide. Typical stoichiometries of microbe growth predict that aerobic bacterial respiration is expected to decrease the total gas partial pressure in solution, while anaerobic bacterial growth or photosynthesis can supersaturate oxygen. For example, if a water is initially at equilibrium with the atmosphere at 25 °C, the total partial pressure will increase above 1 atm from algae photosynthesis: oxygen production outweighs carbon dioxide consumption. Net supersaturation becomes even greater if bicarbonate alkalinity is used as an algal carbon source. Warming of water and decreased local barometric pressure can supersaturate waters, assuming the solutions were initially at atmospheric equilibrium, and dissolved oxygen can also be formed from hypochlorite degradation.

### **Measuring Dissolved Gas(es) Supersaturation**

Measurements of dissolved oxygen via a membrane probe or Winkler method is a common surrogate measure for total dissolved gas supersaturation. This approach is useful and reliable if all dissolved gases are proportionally supersaturated (i.e., air entrainment, ozonation with air as the carrier gas, dissolved air flotation, thermal warming and barometric pressure changes if all gases are initially at equilibrium) or if the water is supersaturated with oxygen (i.e., ozonation with oxygen carrier gas, hypochlorite, photosynthetic algae growth). In contrast, this method is clearly ineffective when oxygen concentrations are not supersaturated but the water is, as in the case of lake aeration or carbon dioxide supersaturation arising from acidification of solutions with inorganic carbon.

A direct measure of dissolved gases in solution is now possible using a total dissolved gas probe (TDGP). Manufactured by only a few companies, the TDGP contains a hollow cylindrical silicon membrane (silastic) that rejects water but allows transfer of dissolved gases from solution until the pressure within the membrane's cavity equals the pressure of gases in solution. The total partial pressure of gases in solution is

displayed digitally, and the instrument can therefore detect gas supersaturation whenever it occurs. If desired, oxygen could be measured with a separate probe and subtracted from the total partial pressure, with various assumptions used to quantify the remaining gases.

There are few drawbacks to the method. Bubbles can form on the silastic membrane and interfere with the TDGP by causing a constant drop in the reported partial pressure, although this can be prevented by pressurizing the sample container. In addition, gases transfer at different rates through the silastic on the TDGP (Table 2). As a result, while it can take about 20 minutes for an accurate measurement of 1.1 atm total pressure from pure nitrogen, the same measurement can be made for carbon dioxide in 5 minutes. Also, carbon dioxide occasionally diffuses through the membrane in momentary excess, requiring additional time for the instrument to stabilize. Certain TDGP's report an erroneously high total gas partial pressure, when the probe is immersed at considerable depth. Once identified, these hydrostatic effects can be corrected.

An alternative form of determining bubble formation potential is the bubble apparatus described by Scardina.<sup>4</sup> This method is advantageous since it is less expensive to build and also has the potential to give a better indication of bubble formation in the treatment plant. However, field testing showed that the apparatus must be submerged in a water bath to prevent errors introduced by changing temperature.

## **Previous Work**

The majority of published research to date on the subject is from consulting firms, contracted by specific utilities to determine feasible degassing strategies and in a few cases to identify the source of dissolve gas supersaturation (Table 3). Care should be taken when reviewing the consulting reports, since numerous errors have been found concerning the fundamental science of bubble formation in treatment plants, as might be expected given the lack of previous research on the subject. The Camp, Dresser, and McKee report for their study of the Metropolitan Water District (MWD) contains a good survey of experiences and studies at other municipalities. Overall, little experimental work has been directed to understanding how various parameters affect the treatment processes.

Table 2 – Gas Diffusion Values in Different Media

	<b>N<sub>2</sub></b>	<b>O<sub>2</sub></b>	<b>CO<sub>2</sub></b>
<b>Velocity in Air (m/s)<sup>9</sup></b>	515	482	411
<b>Diffusion in Water (cm<sup>2</sup>/s)<sup>10,11</sup></b>	1.94x10 <sup>-5</sup>	2.03x10 <sup>-5</sup>	1.9x10 <sup>-5</sup>
<b>Permeability through Silicone (s<sup>-1</sup> (cm Hg)<sup>-1</sup>)<sup>12</sup></b>	227x10 <sup>-10</sup>	489x10 <sup>-10</sup>	3240x10 <sup>-10</sup>

Table 3 – Previous Work on Bubble Formation in Treatment Plants. All Plants Except Shreveport and South Bay Aqueduct Identified Air Entrainment as Source of Gas Supersaturation.

<b>Utility</b>	<b>Project Summary</b>
Boulder, CO	Described degasification alternatives, and pilot tested freefall weir treatment. <sup>13</sup> Investigated vacuum packed towers, heating dearators, and multi cone aerator by Infilco Degremont for degasification. <sup>14*-17</sup>
Denver, CO	Described degasification alternatives and conducted a dissolved oxygen profile through the plant including a pilot filter study on air binding. <sup>18</sup>
MWD	Surveyed air binding at other utilities including site visits, described degasification alternatives, measured profiles of total dissolved gases and dissolved oxygen through plant, measured effects from ozonation, pilot tested freefall weir, paddle wheel, and degasification tower for degasification. <sup>19</sup>
San Diego	Pilot tested effects of various filter submergences, ozonation, and aeration on filter air binding. <sup>8**</sup>
Shreveport	Measured degasification from freefall weir. <sup>20**</sup>
South Bay Aqueduct	Pilot tested the effects of ozonation on coagulation and filtration and tested aeration degasification. <sup>21**</sup>

\* As discussed in reference 15, \*\* As discussed in reference 19

## Materials and Methods

### *Coagulation Study*

Three different levels of dissolved gas supersaturation were created in solution during coagulation tests in a jar apparatus: a water which contained very low dissolved gases, a water saturated with dissolved nitrogen gas, and a water supersaturated with a

specified level of dissolved nitrogen gas. All waters were initially boiled, and solutions termed “low dissolved gases” in this work were sealed and allowed to cool. To saturate and supersaturate solutions, subsamples of this solution were subject to nitrogen gas at pressure, mixed, and measured with a TDGP. Error was always less than 0.005 atm of the target value.

For the coagulation test, one liter 0.01 M sodium nitrate solutions were saturated with gases as desired. These solutions were then dosed with 2.5 or 5 mg/L as Fe from a 0.15 M stock ferric (III) chloride solution, and to maintain pH, 70 and 140  $\mu\text{L}$  of 2 M sodium hydroxide was added just prior to the coagulant, respectively. Due to a smaller atmospheric surface area to volume ratio, one liter Ehrlymer flasks were deemed a better approximation to treatment plants than traditional square jars. Solutions were rapid mixed at 300 rpm for 10 seconds and flocculated at 60 or 100 rpm for 30 minutes using a 3.8 cm Teflon coated magnetic stirbar. Samples were collected at a depth of 3.5 inches from the surface for measurements of settled turbidity.

### *Filtration Study*

All filtration studies were carried out using a mono-media column filter with a circular diameter of 1.5 inches and sand media between the size range 0.417 and 0.589 millimeters as collected by wet sieving (Figure 3). The intermediate material was a mix of 0.125 and 0.25 inches media, and the ballast material was approximately 1 inch in size. The media was thoroughly backwashed prior to each experiment to remove any bubbles and was settled such that initial flow through the filter was always within  $\pm 5\%$  of 3 gpm/ft<sup>2</sup>. A constant head of 6 inches was maintained above the filter at all times, and water entered the filter at 2 inches above the media surface.

The influent was distilled deionized water equilibrated with atmospheric gases. For every 0.1 atm of desired gas supersaturation, 170 mg/L as CaCO<sub>3</sub> alkalinity (added as sodium bicarbonate) was added to the source water, with supersaturation created by acidification to a pH below 4.5 using 1 molar nitric acid. To minimize the amount of gas desorption, the source water was pumped into a 125 mL flask where nitric acid was added, after which the supersaturated water was immediately introduced to the filter.



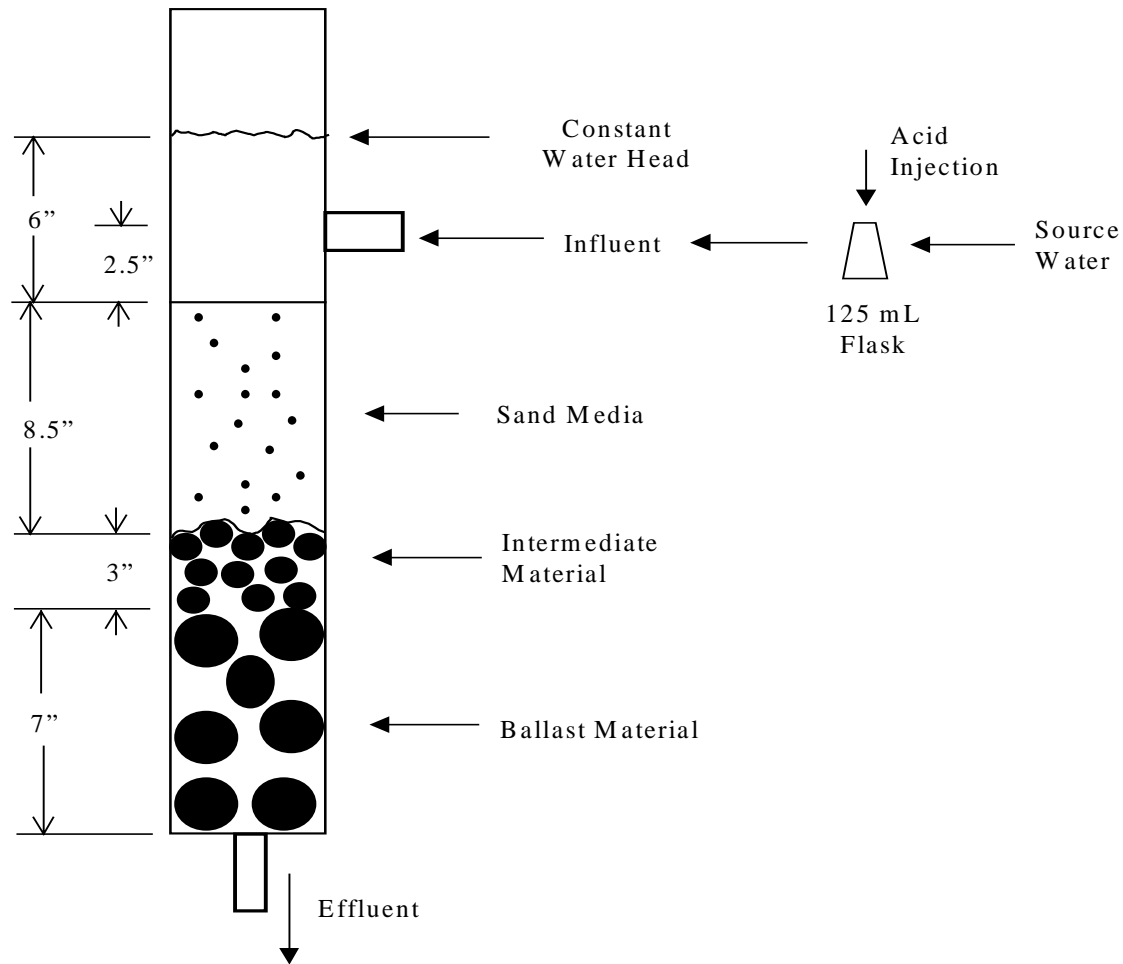


Figure 3 – Pilot Filter Schematic

## Results and Discussion

### *Implications of Bubble Formation in Coagulation*

Despite normal precautions taken to minimize degassing, during the jar test experiment the measured total dissolved gas (TDG) pressure decreased markedly during the rapid mix and flocculation cycles before leveling off (Figure 4). Between the experimental time of 0-5 minutes, the cumulative degassing was due to transferring solution from the pressurized flask to the testing flask, turbulent rapid mixing, and in situ bubble nucleation. Following rapid mixing in the 1.2 atm supersaturated solution, significantly more micro bubbles were seen in solution than in the comparable water saturated with 1.1 atm gas, which undoubtedly led to a greater rate of gas transfer.

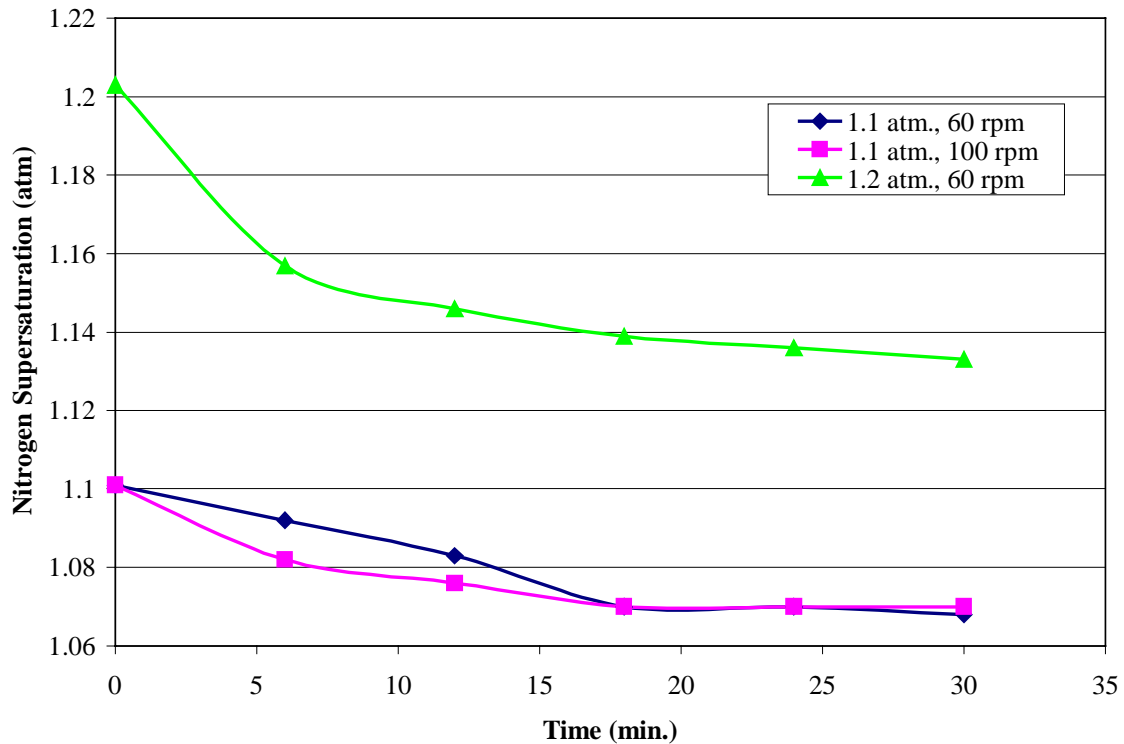


Figure 4 – Extent of Dissolved Nitrogen Supersaturation during Coagulation Experiment

In all scenarios, the solutions containing supersaturated dissolved nitrogen gas exhibited higher measured turbidity during flocculation than the solutions at equilibrium with nitrogen (Figure 5). The increased measured turbidity in supersaturated solutions could have been caused by air bubbles, altered floc particle sizes, or bubbles contributing to measurements of the turbidimeter. The specific cause was not identified in this work. Within minutes of starting flocculation, bubbles began forming on the wall of the flask and on the stirbar in the supersaturated gas solutions. Toward the middle to end of flocculation, bubbles were also attached to the flocs or floating freely in solution (Figure 6). Many of the iron hydroxide flocs had a natural tendency to float at the water surface, and the supersaturated waters typically appeared to have a greater mass of particles at the interface.

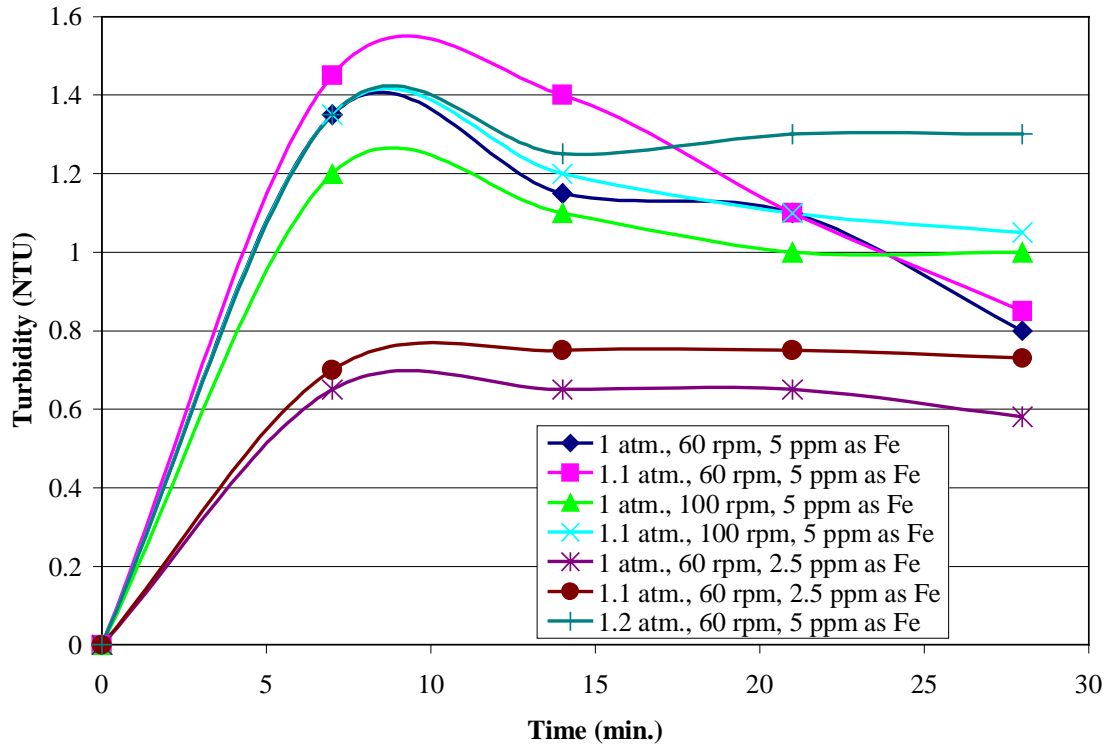


Figure 5 – Turbidity Measurements during Flocculation

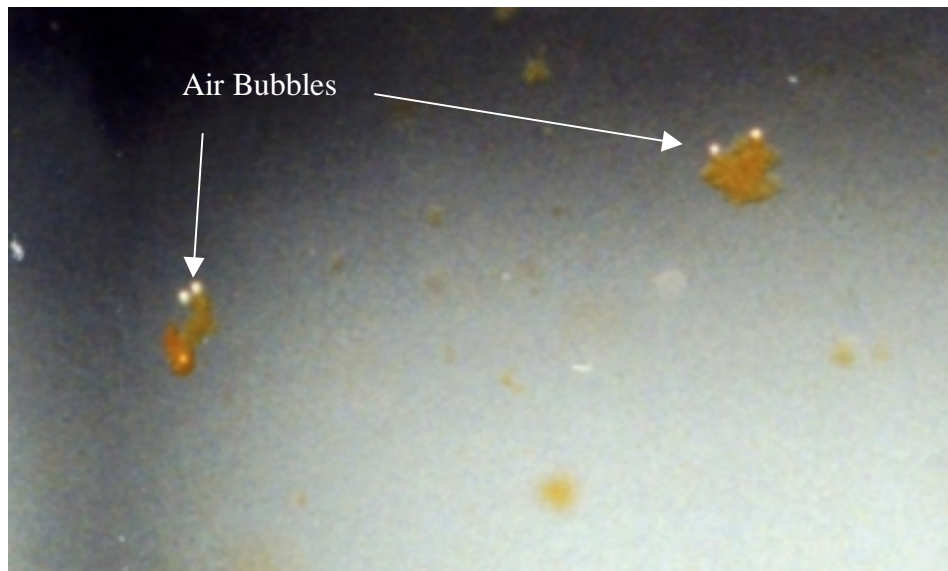


Figure 6 – Bubbles Attached to Floc Particles

During all three tests with a 2.5 mg/L as Fe dose, different agglomerates formed dependent on supersaturation (Figure 7). Solutions that were low in dissolved gases and equilibrated with 1 atm nitrogen had “normal” iron hydroxide particles with a slight yellow-orange color after flocculation. In contrast flocs never formed properly in the solutions saturated with 1.1 atm nitrogen, with only white agglomerates or no flocs visible. The final settled turbidity in the supersaturated solutions were approximately double that of the other solutions at this coagulant dose (Figure 8).

For the solutions coagulated with 5 mg/L Fe, there was a 20% increase in settled turbidity in the 1.1 atm supersaturated solutions when flocculated at 60 rpm compared to the unsaturated waters (Figure 8). This increase was significant at 95% confidence. However, in the same experiment but at 100 rpm flocculation the bubbles were separated from the flocs at the higher mixing rate, and there was no significant difference between the saturated and unsaturated solutions. Tests with a solution at 1.2 atm did not lead to a significant worsening of settled turbidity compared to 1.1 atm solutions, even though the TDG and turbidity were much greater at the end of flocculation in the 1.2 atm waters.

A treatment plant would be expected to respond in a similar manner as the jar tests with only a small percentage of TDG removed between rapid mixing and flocculation. Yet, due to dramatically different areas for gas transfer, a conventional or modified jar test is not very representative of treatment plants (Table 4). It is not possible to know whether this lessened or worsened effects of bubble formation in these experiments relative to treatment plants.

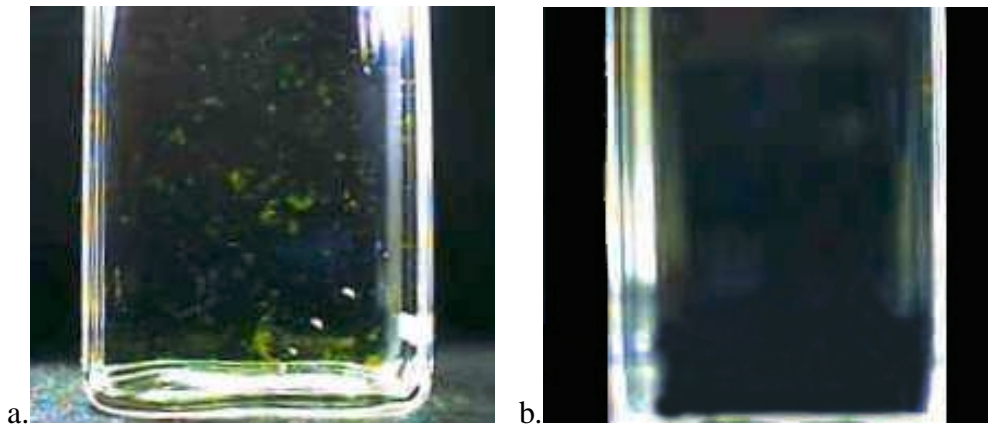


Figure 7 – Comparison of Floc Formation at 2.5 mg/L Fe. Visible Agglomerates in the Solution at Equilibrium with the Atmosphere (a), and No Visible Flocs in the Supersaturated Solution (b).

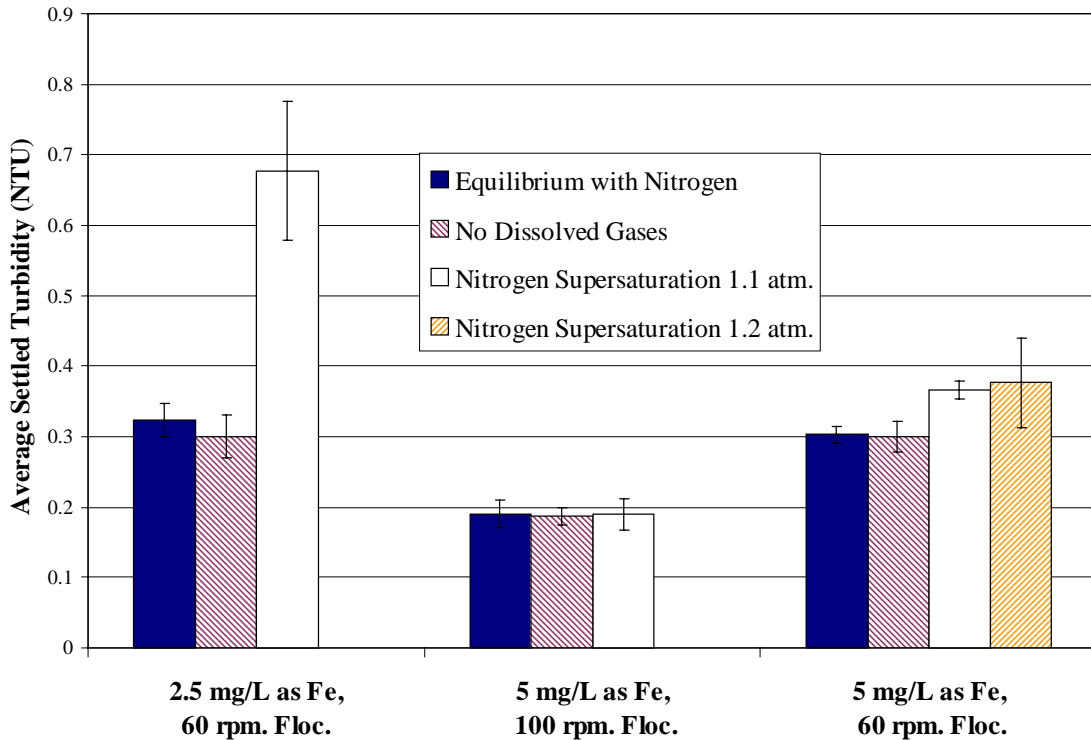


Figure 8 – Final Settled Turbidity for Coagulation Experiments. Error Bars Indicate 95% Confidence. The 2.5 and 5 mg/L Fe solutions settled for 45 and 30 minutes, respectively.

Table 4 – Interfacial Area for Experimental Apparatus versus Full Scale Treatment

Possible Gas Transfer	Surface Area/Volume (cm <sup>2</sup> /L)		
	Erhlymer Flask	Jar Test Beaker	Plant Floc Basin
Atmosphere	20	80	~ 0
Solid Surface of Reactor	405	475	0

Given that dissolved gas supersaturation was proven to have profound effects on coagulation in this study, the question arises whether this phenomenon was influential in previous research results. In the classic study by Amirtharajah on rapid mixing design, solutions were coagulated at different final pHs with alum concentrations at 1-30 mg/L and with initial alkalinity of 80 mg/L as CaCO<sub>3</sub>.<sup>22</sup> The waters were then rapid mixed at either 300, 1000, or 16,000 s<sup>-1</sup> and turbidity measurements were taken following settling. Plotting the settled turbidity in that study after 90 minutes of settling versus the potential bubble formation (calculated for a water initially at equilibrium with the atmosphere) using the model outlined by Scardina<sup>4</sup> illustrates that trends in the Amirtharajah work are

consistent with the observations of this study (Figure 9). That is, settled turbidity increased when bubble formation potential was higher. Rapid mixing at a higher G value markedly improved settling analogous to results in Figure 8, but mixing had nearly no effect on settled turbidity when bubble formation potential was nearly zero.

Similarly, in Chowdury's coagulation experiments at a constant pH 6.5 and coagulant dose, reduced settling occurred when the solution's initial carbonate alkalinity was increased from 0.002 to 0.01 molar.<sup>23</sup> The Scardina model predicts 2.15 and 0.4 mL/L bubble formation potential at 0.01 and 0.002 molar alkalinities, respectively; thus, reduced settling occurred at higher supersaturation as was the case in this work. Even more than 75 years ago, Miller examined effects of alkalinity on coagulation at several doses of alum, and noted that some solutions tested were completely opaque, consistent with micro bubble formation.<sup>24</sup>

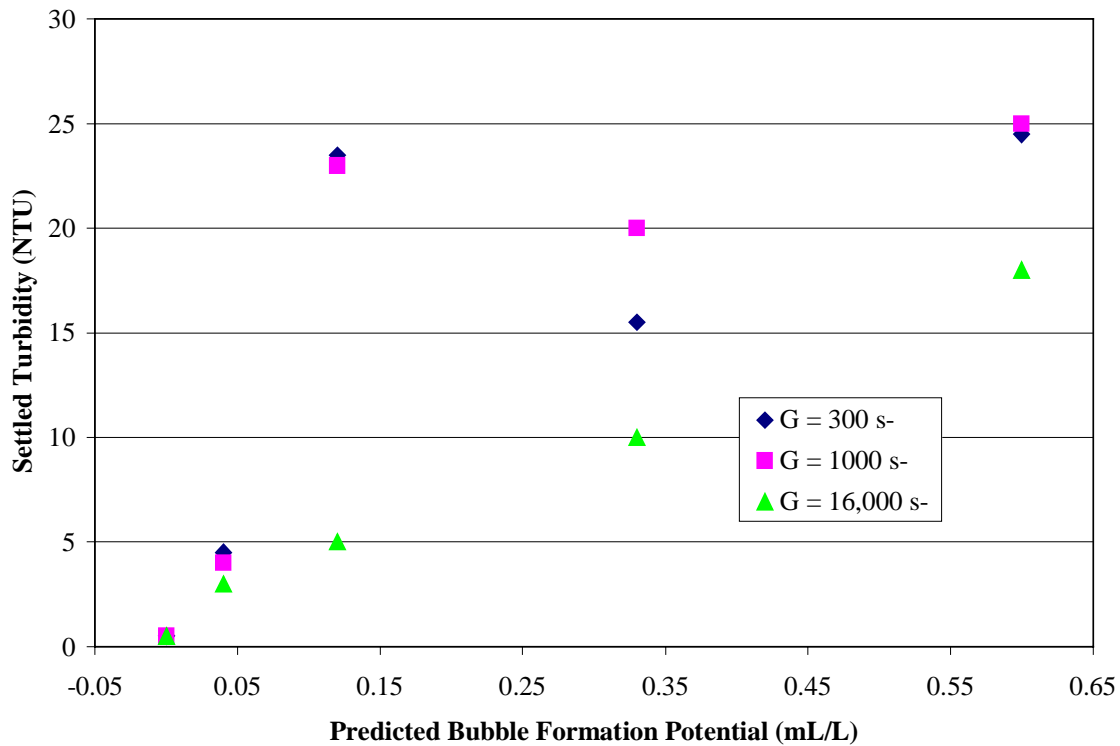


Figure 9 – Relationship between Bubble Formation Potential and Settled Turbidity in the Amirtharajah Study

In sum, while it is uncertain as to the extent to which actual bubbles formed and influenced results in the cited research, it is clear that many phenomena in the literature are consistent with findings from this study and that bubble formation was not considered as a possible cause. Future work should examine the fundamental role of bubble formation in the context of coagulation and flocculation, repeating classic experiments if possible and re-interpreting results if necessary.

### *Implications of Bubble Formation in Filtration*

Supersaturated dissolved gases in treatment plants are expected to interfere with filter performance through a phenomenon known as air binding. In addition to the criteria described earlier that can favor bubble formation, the flow velocity passing through the filter media increases, dropping the hydrostatic pressure and creating a greater driving force for bubble formation, according to Bernoulli's equation:

$$\frac{p}{\lambda} + \frac{V^2}{2g} + z = C$$

In the filtration experiments, it was not determined whether the decreased pressure predicted by Bernoulli's equation increased bubble formation in the filter media.

Bubbles began forming on top of the filter media within a few minutes if the influent was supersaturated at 0.2 atm or greater, and they occasionally detached and floated filter media to the water surface. Most bubbles were observed in the top 0.75 inches of the media, and bubble growth actually pushed the media upward as they grew (Figure 10). In addition, bubbles also formed in the underdrain rocks, with large gas pockets forming and almost completely covering the underdrain at the higher levels of supersaturation tested. This occurrence of bubble formation where space was available is an adaptation to the current theory of air binding, which mainly considered minute bubbles forming between the filter media similar to particles.

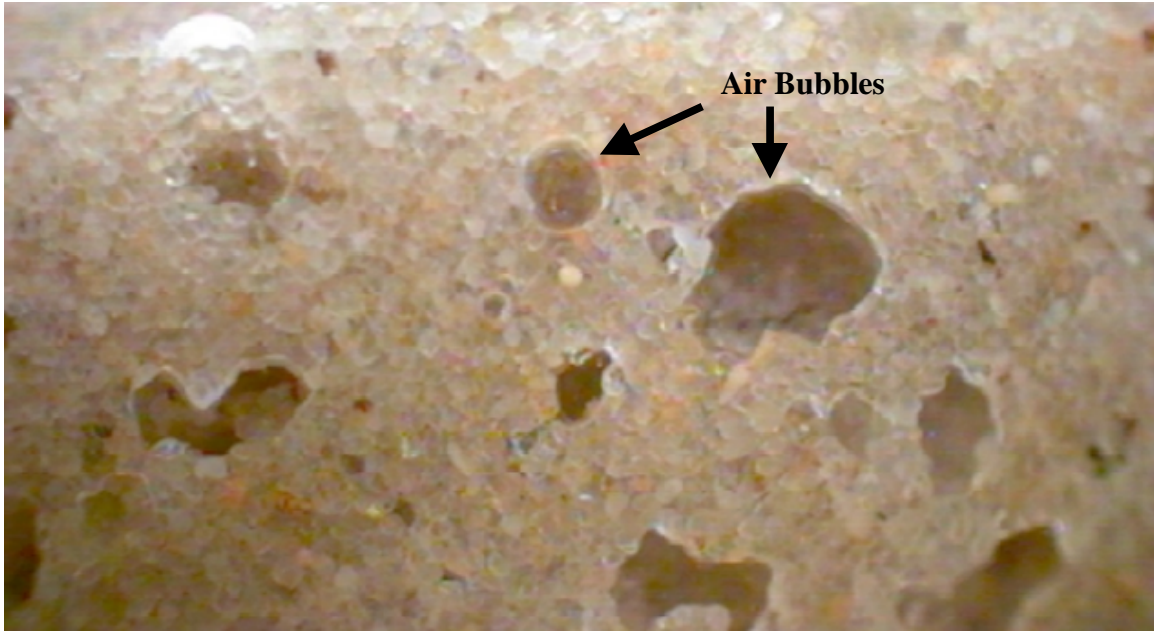


Figure 10 – Air Bubble Formation in Media during Filtration of Supersaturated Waters

The headloss steadily increased in the pilot filter as bubbles grew and restricted flow (Figure 11). The time required to obtain 50% reduction of the initial flow appeared to decrease exponentially with the degree of supersaturation (Figure 12). No significant decrease in flow through the filter occurred in a water at saturation. However, even at 0.05 atm supersaturation, flow was decreased by 50% in 24 hours. Since plants commonly have filter runs between 24-100 hours<sup>25</sup>, the above results suggest that even slight degree of supersaturation can have substantial effects upon headloss.

A rough comparison of the volume of floc and bubbles per liter suggest that such impacts are not surprising. Consider coagulation of a water with 160 mg/L as CaCO<sub>3</sub> alkalinity and raw turbidity of 10 NTU (~70 mg/L bentonite<sup>26</sup> with a specific gravity of approximately 2.65<sup>27</sup>) with 5.8 mg/L as FeCl<sub>3</sub> coagulant to a final pH 7. Assuming all the iron forms flocs with a specific gravity of 1.01, the total volume of particles per liter including associated water is 0.4 mL/L, and it would be expected that most of these particles would be removed in the sedimentation basin. In contrast, if the water was initially at equilibrium with the atmosphere, acidification from the coagulant would lead to a bubble formation potential of 0.3 mL/L. Thus, bubble formation could dominate particle deposition as a source of filter headloss under some circumstances.



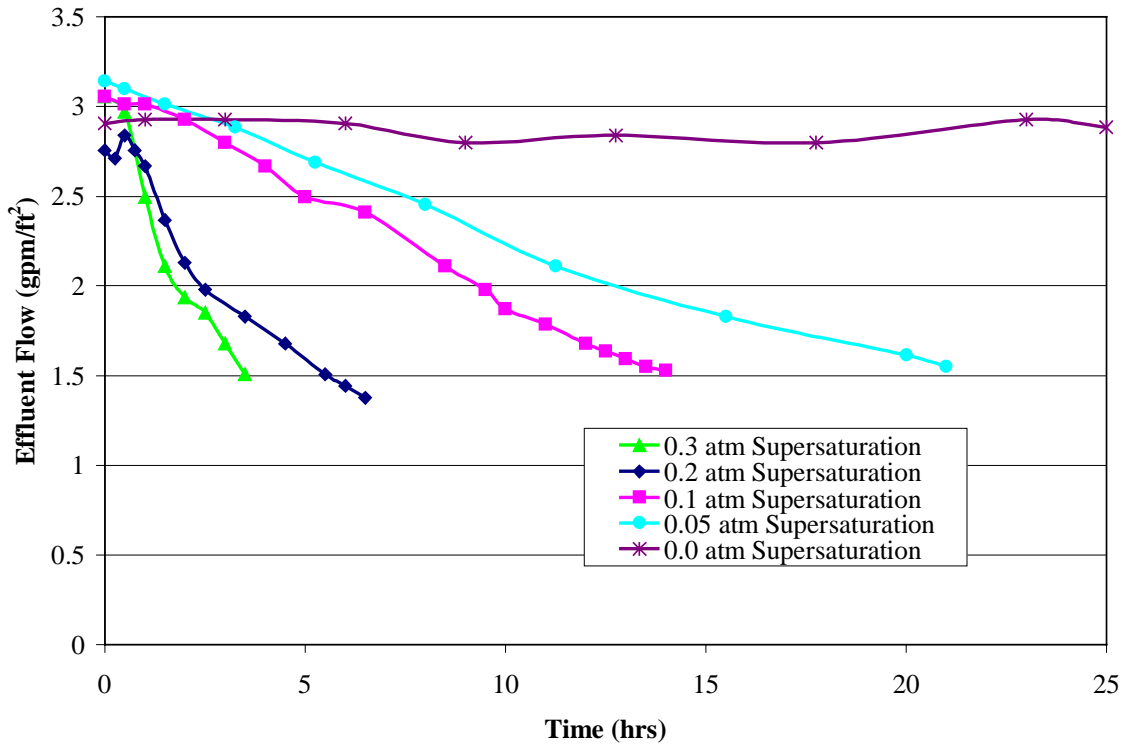


Figure 11 – Effluent Filter Flow at Constant Head

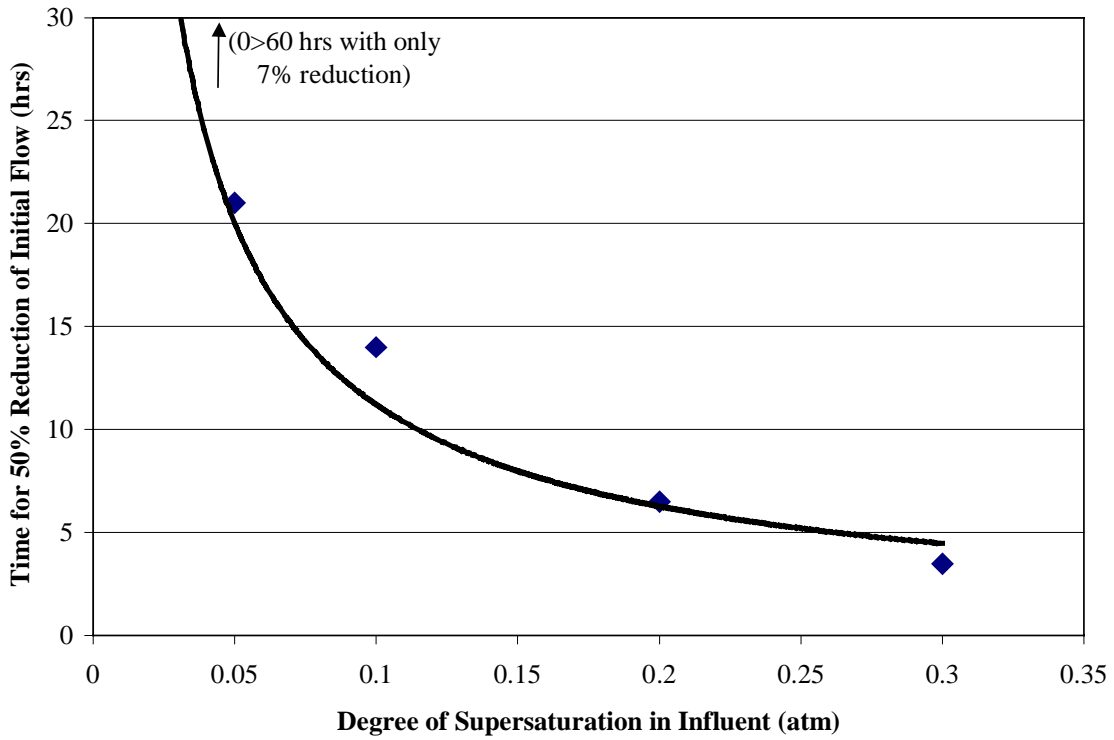


Figure 12 – Time for 50% Reduction of Effluent Flow per Supersaturation

## Water Treatment Plant Case Study

A case study at utility A provided confirmation of key principles developed in the laboratory. The study was conducted at the end of July 1999 when air binding in the filters is most noticeable due to higher plant flows and increased water temperature. This conventional treatment plant has the potential for pre-ozonation but currently only ozonates following sedimentation using air as the carrier gas (Appendix). The raw water has a typical pH of 6.9, 30 mg/L as CaCO<sub>3</sub> alkalinity, 300 color units, and total organic carbon between 20 and 60 mg/L. The water temperature was about 30 °C during sampling. A typical coagulant dose is 150 mg/L of alum, with lime addition to maintain pH at 5.8.

The raw water at the plant during normal operation was slightly undersaturated, but after rapid mixing was at equilibrium with dissolved gases (Figure 13). Total dissolved gases increased to 0.22 atm gauge pressure after post-ozonation, and since the plant usually experiences a zero measured ozone residual due to its reaction with contaminants, diffusion of the carrier gas at depth was assumed the source of supersaturation. Operators believed that filter headloss increased at the plant from bubble formation in sand media, and this was verified by the reduction in total dissolved gases after filtration (Figure 13). These TDG measurements and equations outlined by Scardina<sup>3</sup> for predicting bubble formation, indicate that 1.2 mL of bubbles formed per liter water passed through the filtration process. As the head lowers above the filter for backwashing, bubbles physically boil the media, and the operators let the air release for five minutes prior to initiating backwash flow to help reduce filter media loss (Figure 14). Clearly, bubble formation was causing a serious operational problem at this plant, and the profile in Figure 13 illustrates the power of the TDGP to detect and interpret these phenomena.

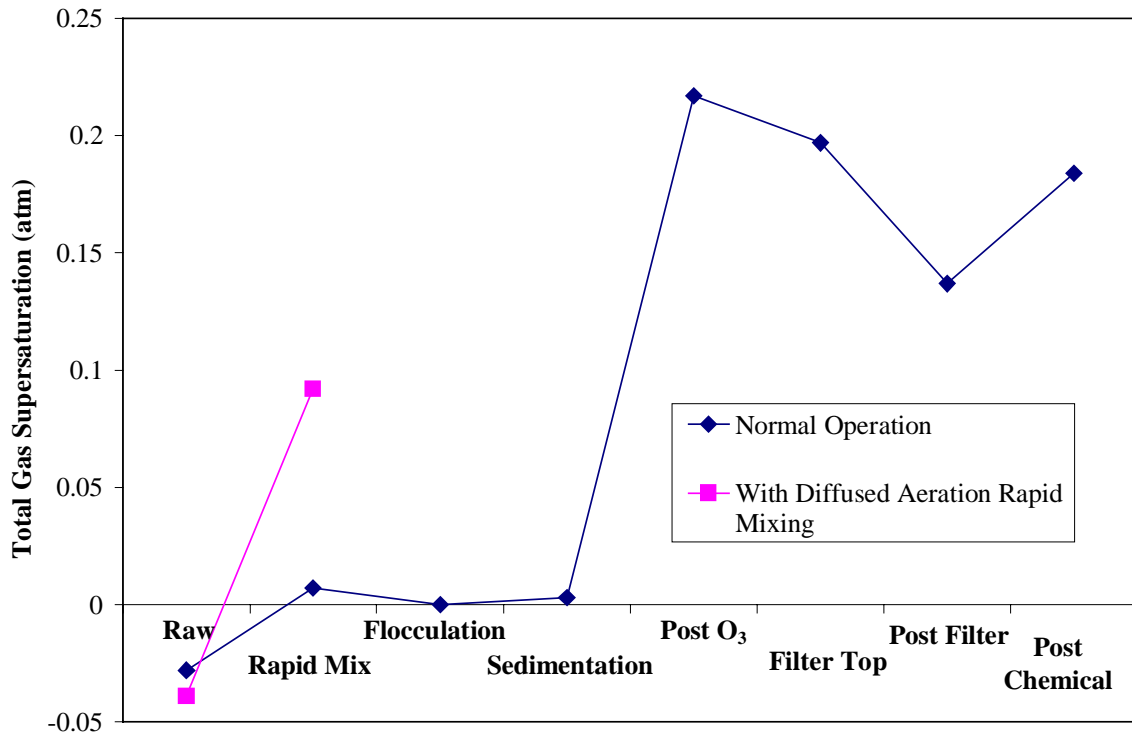


Figure 13 – Total Dissolved Gas Profile through Utility A

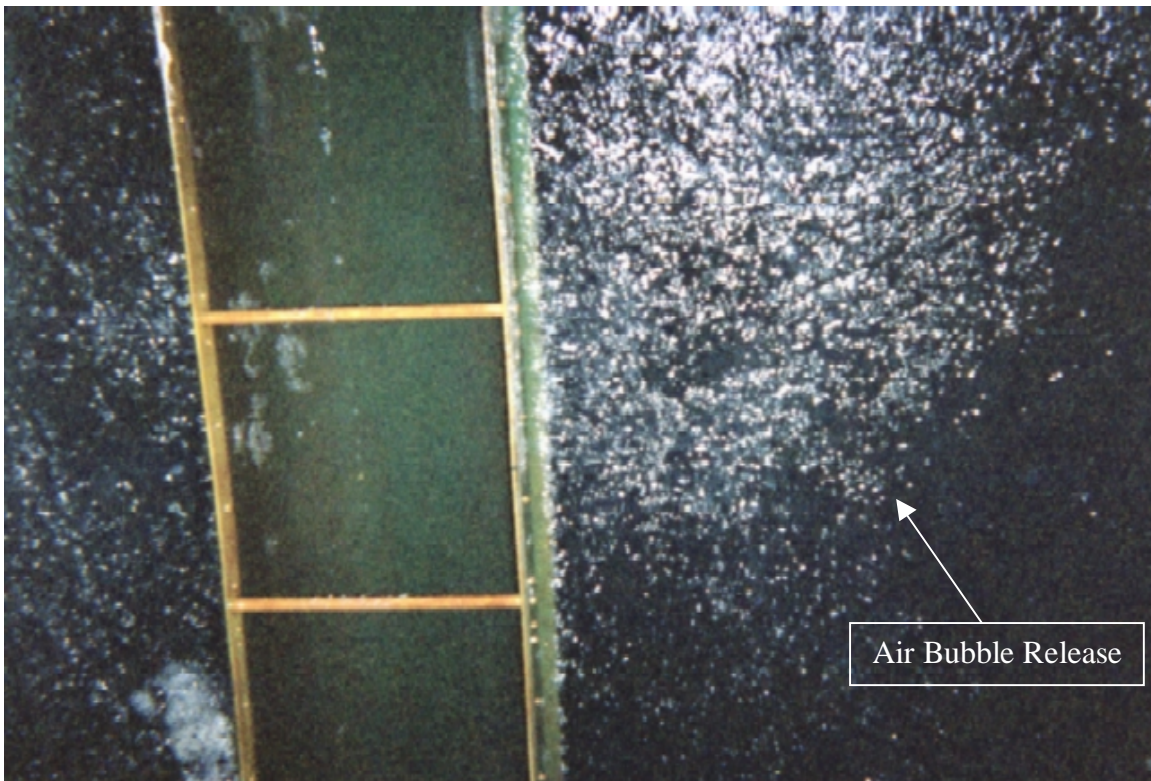


Figure 14 – Air Bubble Release during Filter Backwashing at Utility A

After the sampling event, the operators began diffused aeration in the pre-ozonation cell to rapid mix the coagulant. The aeration at depth increased the partial pressure of dissolved gases from  $-0.039$  to  $0.092$  atm gauge pressure (Figure 13), causing obvious bubble formation in the flocculation basin. Normally with the high coagulant dose, large, fluffy flocs form and settle quickly, and the bottom of the sedimentation basin (15 feet deep) is often visible. With the onset of bubble formation, however, particle agglomeration was hindered, and many agglomerates passed into the filter since settling was impaired. This is consistent with the solids flotation observed from pre-ozonation in the South Bay Aqueduct pilot study<sup>21</sup> and in Figure 7 and 8 of this work. Bubbles were visible on the flocs when samples were taken from the flocculation cell, and when the diffused aeration mixing was terminated, coagulation immediately improved.

## Conclusions

- Sources of dissolved gas supersaturation in water treatment have been documented, and new techniques are described to measure the degree of supersaturation. The TDGP provides important new insights to conventional treatment processes.
- Bubble formation during coagulation and flocculation can potentially inhibit particle sedimentation. In some cases, settled water turbidity was at least double that of a water without supersaturated gases.
- Increasing the degree of supersaturation decreases filter run time, even at  $0.05$  atm supersaturation. Bubble formation in filters can be an important, even dominant, contributor to filter headloss.
- A case study at a water treatment plant confirmed that bubble formation can dramatically decrease operational efficiency in coagulation-flocculation and filtration.

## Acknowledgements

The authors would like to thank the generous anonymous operators at utility A who helped in the case study presented in this work. This work was supported by the National Science Foundation (NSF) under grant BES-9729008. The opinions, findings, conclusions, or recommendations are those of the authors and do not necessarily reflect the views of NSF.

## Notation

[G] = Dissolved gas concentration for a particular gas

$k_h$  = Henry Law's constant for a particular gas

$pG$  = partial pressure of a particular gas

## Appendix. Operational Parameters of Utility A

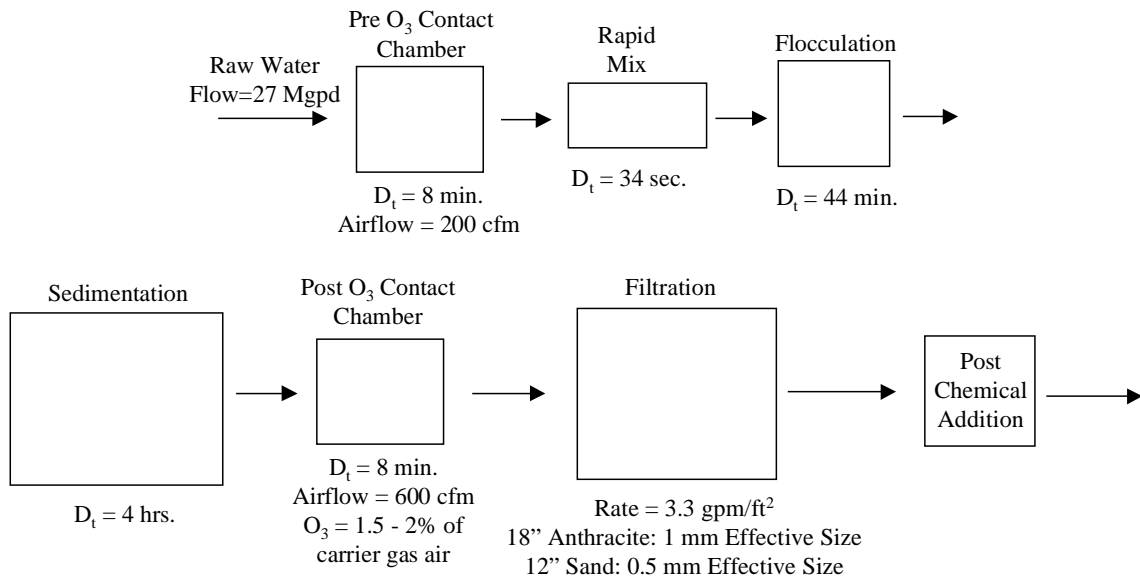


Figure A1 – Schematic of Utility A

## References

1. *Water Quality and Treatment: A Handbook of Community Water Supplies*. Ed., Letterman, R. D. McGraw Hill, Inc. (5<sup>th</sup> ed., 1999).
2. *Model 2100N Laboratory Turbidimeter Instruction Manual*. HACH Company, (1997).
3. Letterman, R. & Shankar, S. Modeling pH in Water Treatment Plants: The Effect of Carbon Dioxide Transport on pH Profiles. Poster at the 1996 AWWA National Conference in Toronto, Canada (1996).
4. Scardina, P. & Edwards, M. Submitted to *Journal of ASCE*. (1999).
5. AWWA. *Ozone in Water Treatment: Application and Engineering*. Eds., Langlais, B., Reckhow, D.A., & Brink, D.R. Lewis Publishers, Michigan (1991).
6. Masters, G.M. *Introduction to Environmental Engineering and Science*. Prentice Hall, New Jersey (1991).
7. Baur, R. "Hypochlorite Problems and Some Solutions." Unified Sewerage Agency Memo.
8. San Diego. Water Quality Report. Report by Powell/Pirnie Assoc. for City of San Diego, CA, (1990).
9. Masterton, W.L. & Hurley, C.N. *Chemistry: Principles and Reactions*. Saunders College Publishing, New York (2<sup>nd</sup> ed., 1993).
10. Baird, M.H.I & Davidson, J.F. Annular Jets II: Gas Absorption. *Chemical Engineering Science*, 17:473 (1962).
11. Thomas, W.J. & Adams. M.J. Measurement of the Diffusion Coefficients of Carbon Dioxide and Nitrous Oxide in Water and Aqueous Solutions of Glycerol. *Transactions of the Faraday Society*, 61:668 (1965).
12. *Lange's Handbook of Chemistry*. Ed. Dean, J.A. McGraw-Hill, Inc., New York (14<sup>th</sup> ed., 1992).
13. Boulder, CO. Reduction of Entrained/Dissolved Air in the Silver Lake Water Supply. Report prepared by CH2M-Hill for Boulder, CO, (1980).
14. Hess, T.F. Removal of Entrained Air from a Source Water. Master thesis, University of Colorado, Boulder, (1980).

15. Boulder, CO. Conceptual Design Memorandum. Report prepared by Richard P. Arber Associates for Boulder, CO, (1993).
16. Boulder, CO. Pilot Vacuum Deaeration Study. Report prepared by Richard P. Arber Associates for Boulder, CO, (1994).
17. Hess, T.F., Chwirka, J.D., & Noble, A.M. Use of Response Surface Modeling in Pilot Testing for Design. *Environmental Technology*, 17:1205, (1996).
18. Denver, CO. Report prepared by HDR Engineering Inc. for Denver, CO, (1997).
19. Metropolitan Water District. Degasification and Filter Air Binding Studies. Report prepared by Camp Dresser & McKee Inc. for Metropolitan Water District of Southern California, (1995).
20. Ferguson, D. & Beuhler, M. Metropolitan Water District of Southern California, Internal Memorandum on Air Binding Data, (1990).
21. Camp Dresser & McKee Inc. South Bay Aqueduct Pilot Plant Studies. Technical Memorandum No. 10, (1990).
22. Amirtharajah, A. & Mills, K.M. Rapid-mix Design for Mechanisms of Alum Coagulation. *Journal of American Water Works Association*, 74:4:210, (1982).
23. Chowdhury, Z.K., Amy, G.L., & Bales, R.C. Coagulation of Submicron Colloids in Water Treatment by Incorporation into Aluminum Hydroxide Flocc. *Environmental Science and Technology*, 25:10:1766, (1991).
24. Miller, L.B. A Study of the Effects of anions Upon the Properties of 'Alum Flocc.' (1925).
25. Montgomery, J.M. *Water Treatment Principles and Design*. (1985).
26. Tseng, T. Considerations in Optimizing Coagulation. Master thesis, University of Colorado, Boulder, (1997).
27. Ojha, C.S.P. & Graham, N.J.D. Theoretical Estimates of Bulk Specific Deposit in Deep Bed Filters. *Water Research*, 27:3:377, (1993).

## **AUTHOR'S VITA**

### **Robert Paolo Scardina**

Paolo Scardina was born on October 21, 1975 in Columbus, Ohio, and was raised in the backwoods of West Virginia. In addition to completing his Master's Degree in Environmental Engineering at Virginia Tech, Paolo also holds a Bachelor of Science Degree in Mining and Minerals Engineering from Virginia Tech, Blacksburg, Virginia. Paolo plans to pursue his doctorate in the same area of study at Virginia Tech.